Acta Otolaryngol (Stockh) 1993; 113: 591–597

Spontaneous Cellular Vibrations in the Guinea-Pig Cochlea

S. E. KEILSON,[1]* S. M. KHANNA,[2] M. ULFENDAHL[3] and M. C. TEICH[4]

From the Departments of [1]Applied Physics and [2]Otolaryngology, Columbia University, New York, USA, [3]Department of Physiology II, Karolinska Institutet, Stockholm, Sweden and [4]Departments of Applied Physics and Electrical Engineering, Columbia University, New York, USA

Keilson SE, Khanna SM, Ulfendahl M, Teich MC. *Spontaneous cellular vibrations in the guinea-pig cochlea.* Acta Otolaryngol (Stockh) 1993; 113: 591–597.

Mechanical vibrations of Hensen cells were measured with a laser-heterodyne interferometer in the third turn of the guinea-pig temporal-bone preparation without the application of an external stimulus. Smoothed periodograms (spectral-density estimates vs frequency) were constructed from the velocity vs time waveforms recorded from individual cells. For some cells, several peaks appear in the periodograms at levels as high as 10 dB above the noise floor, indicating the presence of spontaneous vibrations. The frequencies at which the peaks are located differ in different preparations, indicating that the observed peaks are not caused by the presence of ambient noise or ambient vibrations. It is demonstrated that smoothed-periodogram analysis is superior to fast-Fourier-transform analysis for discerning these spontaneous spectral components. The frequency tuning curves of cells from which spontaneous vibrations were measured (determined by applying an external stimulus to the ear) have single principal peaks. When the spontaneous spectral features are present, their frequencies lie, for the most part, within the principal-peak region of the tuning curve. We propose that these spontaneous vibrations originate at the outer hair cells and are the source of spontaneous otoacoustic emissions in the ear. *Key words: spontaneous otoacoustic emissions, guinea pig, cochlear micromechanics, cochlea.*

INTRODUCTION

Spontaneous otoacoustic emissions are weak, narrowband acoustic signals emitted from the ear in the absence of an external stimulus. The presence of these emissions has been established in man and in a variety of animals (1–6). They are most prevalent in the 2-kHz region, although they have been observed at frequencies as high as 8 kHz. Their amplitude is generally less than 20 dB:SPL.

Kemp (2) postulated that the presence of otoacoustic emissions may be related to the active amplification process in the cochlea, when the positive-feedback mechanism is out-of-control. Zenner (7) suggested that otoacoustic emissions result from active mechanical processes in the outer hair cells of the cochlea. An analysis of otoacoustic emissions led Talmadge et al. (8) to conclude that they originate from a self-sustaining oscillator. It has also been proposed that otoacoustic emissions may be related to the motile properties of outer hair cells (4); indeed, the length changes of isolated outer hair cells in response to chemical, electrical, and acoustical stimuli have been described by a number of research groups (9–11). Spontaneous mechanical fluctuations have previously been seen in isolated turtle cochlear ciliary bundles, but not from the reticular lamina of these cells (12), and "excess spontaneous motion" was observed in the hair bundle of one frog saccular cell (13).

In the region of the third turn of the guinea-pig cochlea, where our vibration measurements were made, outer hair cells and Hensen cells display mechanical tuning with characteristic frequencies in the range between 500 and 1,000 Hz. In addition to this ac tuning, the lengths of these cells change when sound is applied to the ear. This length-change response is sharply tuned and is thought to be produced by the motile response of the outer hair cells, as has been demonstrated in the isolated-cell preparation (11). A shift in the position of the reticular lamina has been observed in the third turn of the intact guinea-pig temporal-bone preparation as well (14), and it is believed to result from cell motility. At a given place in the cochlea, the characteristic frequency of the displacement response and the ac tuning is the same (14), but the displacement response is more sharply tuned.

In view of these observations, it is important to determine whether sensory cells vibrate spontaneously and whether these vibrations are the underlying source of spontaneous otoacoustic emissions (SOAEs). To make this determination, we measured the time course of the velocity vibrations of Hensen cells in the third turn of a fresh guinea-pig temporal-bone preparation with no stimulus applied to the ear. It is known that Hensen cells are tightly coupled to outer hair cells (15) so that the vibrations of outer hair cells will be seen at the Hensen cells. The reflectivity of Hensen cells is substantially higher than that of other cells in the cochlea, allowing us to measure the spontaneous vibrations near the noise threshold. Our spontaneous velocity measurements were carried

* Current address: Center for Hearing Sciences, Johns Hopkins University, Baltimore, Maryland, USA

out using unaveraged data that was collected over relatively long periods of time.

The use of a nonparametric signal-analysis scheme was necessary to detect whatever natural frequency components might be present in the velocity waveform. In this paper, we show how the smoothed (and averaged smoothed) periodogram can be used to provide a reduced-variance estimate of the spectrum for the velocity vibrations of Hensen cells. The spectra measured from the cells that exhibited such vibrations were found to consist of a number of spectral components that were as large as 10 dB above the noise floor. The number of spectral components, and their frequencies, differed in different preparations.

In a companion paper (16), we address questions concerning the stability of the observed cellular vibrations, the tradeoff between confidence interval and bandwidth of the velocity spectral density estimate, and the relation between the frequency tuning curve and the velocity spectral density estimate. Some of the spontaneous spectral components observed in the periodogram are located in the principal-peak region of the frequency tuning curve whereas others are located in the tail region (16).

Our findings, in preliminary form, were reported at the two most recent annual meetings of the Association for Research in Otolaryngology (17, 18).

MATERIAL AND METHODS

The general method of recording cellular vibrations in the cochlea has been described in detail elsewhere (15). The measurements were made in the third turn of the left temporal-bone preparation (in the region between 13.2 and 17.5 mm from the base of the cochlea) obtained from pigmented guinea pigs with positive Preyer reflexes. The right temporal bone was used for different experiments. Experiments were carried out on 24 animals.

The apex of the cochlea was opened and the fourth turn was removed. The preparation was immersed in a plexiglass tank filled with tissue-culture medium (MEM) through which oxygen was bubbled. An objective lens (Olympus 20 ×), with a custom-made dipping cone inserted in the wall of the tank through a watertight circular opening, was utilized for viewing the cochlea with the optical sectioning microscope and for measuring the cellular vibrations with the heterodyne interferometer. The heterodyne interferometer, which is integrated with the optical sectioning microscope, can measure the vibration of an object on which the microscope is focused, provided that the carrier-to-noise ratio is sufficiently high (15). The 2-μm-diameter laser spot on the object, seen through the microscope eyepiece, can be placed on a selected cell by moving the temporal bone with an x-y-z micropositioning system (15).

To measure the frequency tuning curve, sound was applied to the ear via a plastic tube connected to an acoustic driver. A flexible plastic probe tube, placed with its tip within 1 mm of the tympanic membrane, was used to measure sound pressure levels. The sinusoidal electrical signal applied to the acoustic driver was generated using a 386-based computer system coupled to a 16-bit D/A converter. The interferometer response was passed through an anti-aliasing filter, a 16-bit A/D converter, and then stored in the hard disk of the computer system. Details of the digital signal processing have been described earlier (15).

The smallest vibration amplitudes can be measured with the interferometer only when the carrier-to-noise ratio is high. This situation prevails when the microscope is focused on a Hensen cell because of its high reflectivity. (The carrier-to-noise ratio during the measurements reported here was about 55 dB, measured in a 150-kHz bandwidth.) Thus far, it has only been possible to detect spontaneous vibrations at Hensen cells.

The interferometer utilized optical sectioning with a sectioning depth of about $\pm 5\,\mu$m. The light reaching the photodetector in the interferometer originates principally from a volume of tissue about 2 μm in diameter and 10 μm in depth. This volume is far smaller than that of individual sensory cells in the cochlea so that the vibrations were recorded from small regions of single cells.

With the microscope and interferometer focused on a selected Hensen cell, mechanical vibrations were measured with and without an acoustic stimulus applied to the tympanic membrane. The data samples were obtained at 40-μs intervals. In the presence of the stimulus, the response was averaged 25 times in a buffer consisting of 1,024 bins. For measuring the spontaneous response, no external stimulus was generated and the interferometer output was stored in 4,096 bins. A set of successive (unaveraged) responses was obtained. In later experiments, longer sequences of the unaveraged response were stored in $128 \times 1{,}024 = 131{,}072$ bins, each 40-μs long.

The magnitude (or squared magnitude) of the discrete Fourier transform (DFT) is often an inadequate measure of the spectral components contained in a signal. In the absence of an external stimulus we require an optimal nonparametric signal-analysis scheme that reveals whatever natural frequency components may be present when *a priori* knowledge about the signal is not available (19). This task requires the use of a procedure for estimating the autocovariance function (i.e., the zero-mean autocorrelation function) of the signal, or its Fourier

transform (called the spectrum or periodogram). The Fourier-transform-pair relationship between the autocovariance function and the periodogram is the well-known Wiener-Khinchin theorem (20).

The original time series is first modified to incorporate data tapering and zero-padding (19–21). Data tapering reduces the high-frequency components artificially introduced by the arbitrary sharp turn-on and turn-off of a finite data stream, which can result in erroneous high-frequency content that distorts spectral density estimates at other frequencies. The specific data tapering that we used takes the form $[1 - \cos(n\pi/10)]/2$ for the first ten bins, and its mirror image for the last 10 bins, where $0 \leqslant n \leqslant 10$. Zero-padding extends the data stream with added zeros and is traditionally used to improve frequency resolution or to bring the size of an array up to a power of 2 for the fast-Fourier-transform (FFT) algorithm. It also prevents wrap-around and end-effect problems, which result from the periodic nature of the signal in discrete convolution. This occurs when calculating the autocovariance estimate by taking the discrete inverse transform of the squared magnitudes of the DFT. The array needs to be padded with zeros only up to the lag value of the autocovariance function of interest to get correct sample values. If no temporal lag window is applied, zero-padding is not necessary for this purpose.

There are a number of ways of implementing periodogram calculations (19–21). One computational approach for achieving a spectral density estimate with low variance is to average neighboring frequency spectral estimates with a specified window function. The result is a smoothed periodogram, which comes at the cost of reduced frequency resolution. In our implementation, the data is first subjected to an FFT and the square magnitude of the complex frequency components is calculated. The result is then inverse-transformed back into the time domain, whereupon the temporal data may be properly regarded as an estimate of the autocovariance function. A temporal smoothing or window function (e.g., a Bartlett window) is then applied to this time function which, when transformed into the frequency domain, becomes the reduced variance estimate of the spectral density (20). We collected long streams, as well as successive multiple sets, of spontaneous vibration data. This enabled us to further reduce the variance of the spectral estimate by averaging the smoothed periodograms.

RESULTS

Hensen cells from six of the 24 animals studied exhibited spontaneous velocity vibrations. Periodograms from two of these, representative of the subset of six, are presented below.

The smoothed periodogram is superior to the FFT for providing a spectral estimate because of the inherent spectral smoothing. This is illustrated in Fig. 1. The squared magnitude of the FFT of an unaveraged set of velocity data is presented in Fig. 1*a*. The estimate is provided in dB with a reference level of 1 cm^2/s^2. The number of bins is N = 4,096, each with a width of 40 μs. A rectangular window with L = 2,048 bins was used. The bandwidth, representing the frequency resolution associated with this window, is 6 Hz. The 80% confidence interval for the estimate, which in this case is 22.3 dB, is indicated by the solid black vertical bar. The squared magnitude of the FFT is seen to be highly noisy and it is difficult to discern the presence of spectral peaks.

The single smoothed periodogram for this same data set is shown in Fig. 1*b*. The number of bins is N = 3,072, each with a width of 40 μs. A Bartlett window with L = 1,024 bins was used, and the remaining 1,024 bins were zero-padded. The bandwidth, representing the frequency resolution associated with this window, is 37 Hz. Data tapering was incorporated. The 80% confidence interval for the estimate in this case is 7.6 dB, which is sufficiently reduced in comparison with that for the squared magnitude of the FFT, that several natural peaks between 100 and 200 Hz, and between 600 and 1,200 Hz, can be seen. The reduction of the confidence interval from 22.3 dB to 7.6 dB comes at the expense of an increase in the frequency resolution (bandwidth) from 6 Hz to 37 Hz.

Fig. 1*c* reveals the advantages of further variance reduction, obtained by averaging periodograms to obtain the averaged smoothed periodogram. In this case, 174 single smoothed periodograms, such as the one represented in Fig. 1*b*, have been averaged together. The bandwidth, representing the frequency resolution associated with this window, is again 37 Hz but the 80% confidence interval is now reduced to a tiny 0.5 dB. Five spectral peaks can now be clearly discerned; these are located at 128, 201, 574, 732, and 952 Hz (the highest subpeak of the spectral feature). (Frequencies are specified as those digital bins containing the largest local velocity spectral density.) The three highest frequency peaks lie in the vicinity of the characteristic frequency of the cell, which is 659 Hz.

In a companion paper we show that the same frequencies are obtained from smoothed periodograms calculated from 5 nonoverlapping subsets of the long time series collected for this cell (16). The frequency tuning curve for the cell was measured using a sinusoidal sound stimulus applied to the

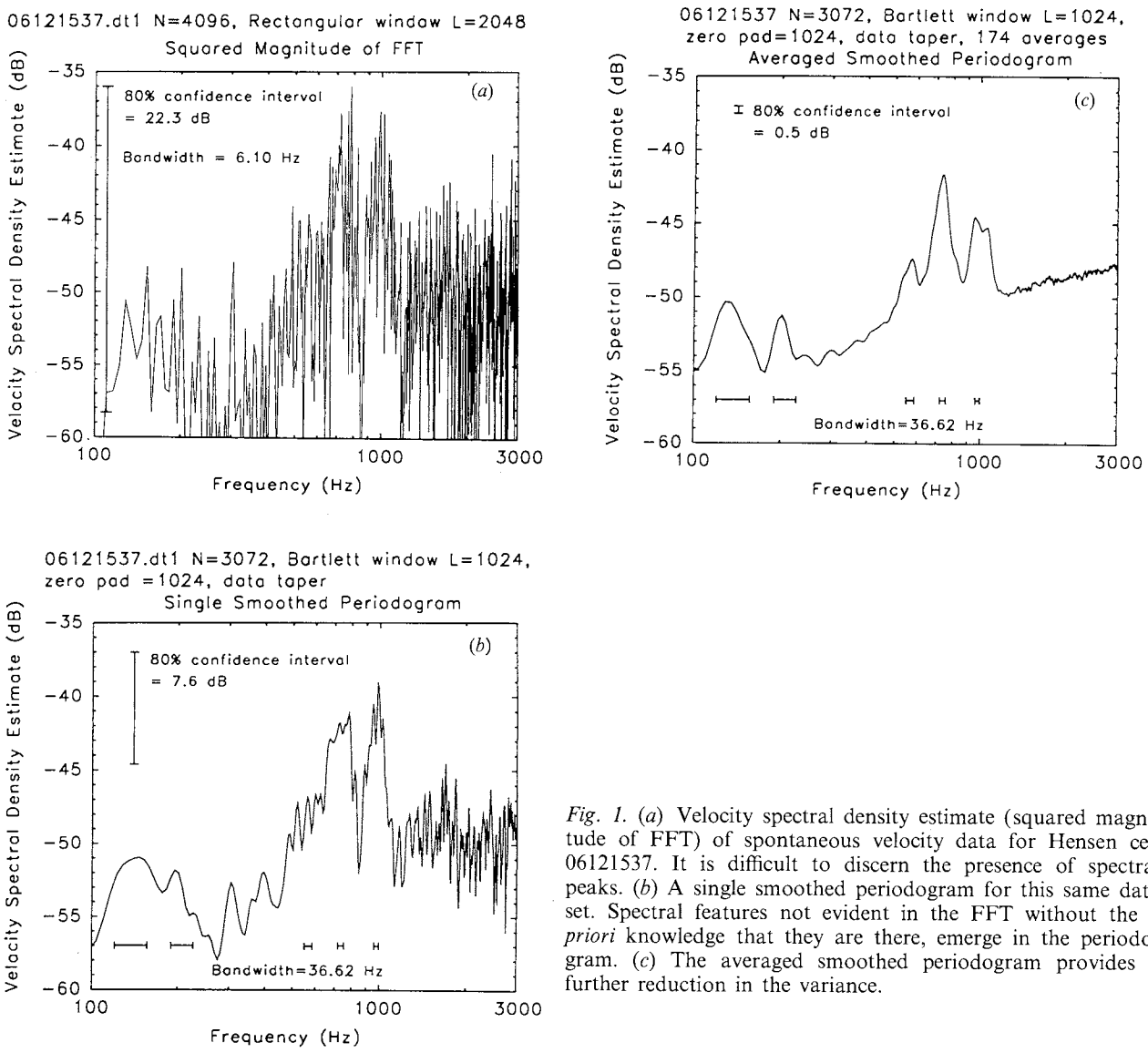

Fig. 1. (*a*) Velocity spectral density estimate (squared magnitude of FFT) of spontaneous velocity data for Hensen cell 06121537. It is difficult to discern the presence of spectral peaks. (*b*) A single smoothed periodogram for this same data set. Spectral features not evident in the FFT without the *a priori* knowledge that they are there, emerge in the periodogram. (*c*) The averaged smoothed periodogram provides a further reduction in the variance.

external ear with steps of 24 Hz. This resolution is sufficiently high so that additional peaks would have appeared in the principal tuning curve were they present.

Fig. 2 illustrates the same sequence for another Hensen cell exhibiting spontaneous vibrations, this one with a characteristic frequency of 562 Hz. Fig. 2*a* shows the squared magnitude of the FFT of an unaveraged set of velocity data. Again, the presence of spectral peaks cannot be readily discerned. Fig. 2*b* shows the single smoothed periodogram for this same data set. Several spectral peaks appear to be present. The averaged smoothed periodogram for this cell, shown in Fig. 2*c*, clearly reveals five peaks located at 134, 201, 623, 744, and 989 Hz. The 80% confidence interval in this case is reduced to 0.7 dB since 130 averages were available. Again, the three highest-frequency peaks are in the vicinity of the characteristic frequency of the cell. The frequencies of the peaks differ for the two cells.

DISCUSSION

The smoothed periodogram method of spectral analysis is particularly useful for revealing hidden periodicities, such as those shown in Figs. 1*c* and 2*c*. Multiple, relatively narrow, spectral components are evident in the spontaneous response of some Hensen cells located in the third turn of the guinea-pig temporal-bone preparation.

The amplitudes of the peaks in the periodogram substantially exceed background noise levels. Some of the spontaneous spectral components are located within the frequency region of principal tuning of the cell, but they are far sharper than the frequency tuning curve itself. The spontaneous vibrations in the

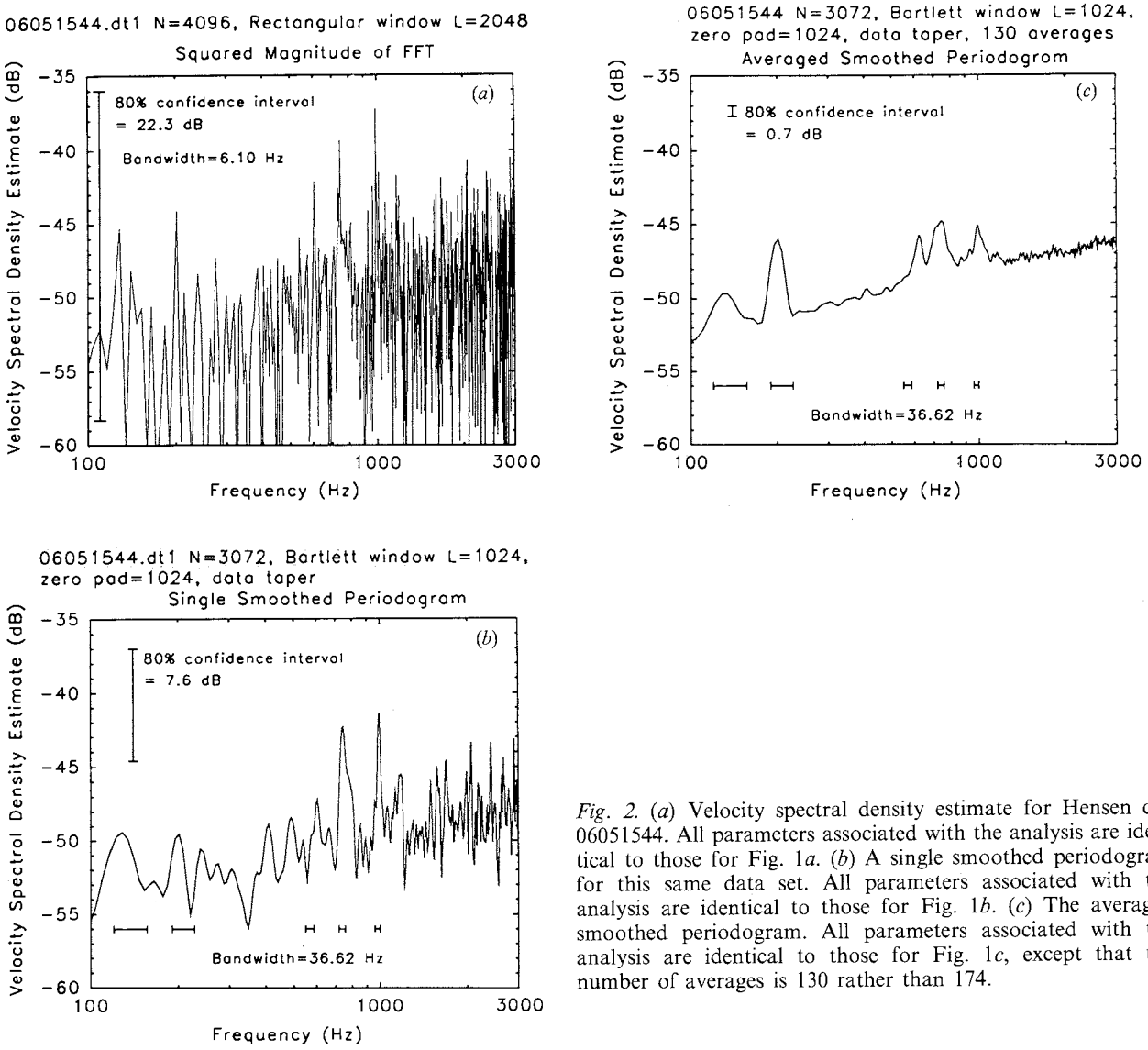

Fig. 2. (*a*) Velocity spectral density estimate for Hensen cell 06051544. All parameters associated with the analysis are identical to those for Fig. 1*a*. (*b*) A single smoothed periodogram for this same data set. All parameters associated with the analysis are identical to those for Fig. 1*b*. (*c*) The averaged smoothed periodogram. All parameters associated with the analysis are identical to those for Fig. 1*c*, except that the number of averages is 130 rather than 174.

periodogram therefore do not arise from filtered noise (which would have a single principal peak). Furthermore, these peaks cannot arise from external sources, such as mechanical vibrations of the components, or sound leaking in from outside the chamber, since they are present only in fresh preparations and their frequencies differ in different preparations.

These peaks could be produced by the vibrations of several outer hair cells that couple to the point of measurement. Although we believe that the origin of these spontaneous vibrations is at the outer hair cells, we have thus far been unable to measure the vibrations directly from these cells because their optical reflectivity is low (15).

Our results demonstrate that some sensory cells in the cochlea vibrate spontaneously; these vibrations are likely related to otoacoustic emissions. It is therefore of interest to compare the characteristics of the spontaneous cellular vibrations we have measured with those of spontaneous otoacoustic emissions: *i)* In our experiments, the spontaneous vibrations were measured in the guinea-pig temporal-bone preparation. SOAEs have been observed from guinea-pig ears by Evans et al. (22) and by Ohyama et al. (23, 24). *ii)* Our periodograms show multiple peaks of different strengths. Multiple-peaked SOAEs are common (25). *iii)* In the region of the third turn of the cochlea, where our measurements were conducted, characteristic frequencies range from 500 to approximately 1,000 Hz. The spectral components of the spontaneous cellular vibrations also lie in this range. Indeed, spontaneous otoacoustic emissions observed in the ear canal are also usually in the 1–2 kHz region (6, 23). One possible reason for the preference for this frequency

range is that the reverse coupling between the malleus and the tympanic membrane is poor at high frequencies. Since the SOAEs are only about 15 dB above the noise floor, a loss of even 10 dB in coupling would be sufficient to make them unobservable. *iv)* The noise floor of our periodogram measurement in Fig. 1*c* (with 174 averages and a bandwidth of 37 Hz) is equivalent to about −4 dB:SPL; the largest peak of the spontaneous vibrations is equivalent to about +7 dB:SPL. These values are comparable with those of SOAEs (6). *v)* Spontaneous cellular vibrations are observed in about 25% of the preparations we examined and the width of the largest peak was approximately 90 Hz. Spontaneous otoacoustic emissions in guinea pigs were observed by Ohyama (23, 24) in 21% of the animals tested. The maximum level of emissions was 26.8 dB:SPL, and the average level was 12.1 dB:SPL. The width of the spectrum at a point −6 dB with respect to the peak was in the range 30–50 Hz. Our observations are therefore not dissimilar from those of Ohyama.

In summary, we have found that the temporal-bone preparation, together with laser-heterodyne interferometry and a nonparametric signal-analysis scheme, has made it possible to study extremely small vibrations directly at the cellular level. Measurements such as these may elucidate the mechanisms involved in spontaneous otoacoustic emissions and could provide a means for assessing the physiological condition of individual cells in the cochlea. We are in the process of investigating further what characteristics of a particular experiment might correlate with the observation of such vibrations.

ACKNOWLEDGEMENTS

This work was supported by the Office of Naval Research under Grant N00014-92-J-1251, NIDCD Program Project Grant DC00316, the Emil Capita Foundation, the Swedish Medical Research Council, the Söderberg Foundation, and the Foundation Tysta Skolan.

REFERENCES

1. Kemp DT. Evidence of mechanical nonlinearity and frequency-selective wave amplification in the cochlea. Arch Otorhinolaryngol 1979; 224: 37–45.
2. Kemp DT. Physiologically active cochlear micromechanics—one source of tinnitus. In: Evered D, Lawrenson G, eds. Tinnitus. London: Pitman, 1981: 54–81.
3. Wit HP, Ritsma RJ. Evoked acoustical responses from the human ear: some experimental results. Hear Res 1980; 2: 253–61.
4. Plinkert PK, Gitter AH, Zenner HP. Tinnitus associated spontaneous otoacoustic emissions. Acta Otolaryngol (Stockh) 1990; 110: 342–7.
5. van Dijk P, Wit HP. Amplitude and frequency fluctuations of spontaneous otoacoustic emissions. J Acoust Soc Am 1990; 88: 1779–93.
6. Zurek PM. Acoustic emissions from the ear: a summary of results from humans and animals. J Acoust Soc Am 1985; 78: 340–4.
7. Zenner HP. Modern aspects of hair cell biochemistry, motility and tinnitus. In: Feldmann H, ed. Proc Third International Tinnitus Seminar, Münster. Karlsruhe: Harsch-Verlag, 1987: 52–7.
8. Talmadge CL, Tubis A, Wit HP, Long GR. Are spontaneous otoacoustic emissions generated by self-sustained cochlear oscillations? J Acoust Soc Am 1991; 89: 2391–9.
9. Brownell WE, Bader CR, Bertrand D, de Ribaupierre Y. Evoked mechanical responses of isolated cochlear outer hair cells. Science 1985; 227: 194–6.
10. Zenner HP, Zimmermann U, Schmitt U. Reversible contraction of isolated mammalian cochlear hair cells. Hear Res 1985; 18: 127–33.
11. Brundin L, Flock Å, Canlon B. Sound-induced motility of isolated cochlear outer hair cells is frequency-specific. Nature 1989; 342: 814–6.
12. Crawford AC, Fettiplace R. The mechanical properties of ciliary bundles of turtle cochlear hair cells. J Physiol (Lond) 1985; 364: 359–79.
13. Denk W, Webb WW, Hudspeth AJ. Mechanical properties of sensory hair bundles are reflected in their Brownian motion measured with a laser differential interferometer. Proc Natl Acad Sci USA 1989; 86: 5371–5.
14. Brundin L, Flock Å, Khanna SM, Ulfendahl M. Frequency-specific position shift in the guinea pig organ of Corti. Neurosci Lett 1991; 128: 77–90.
15. ITER. Cellular vibration and motility in the organ of Corti. Acta Otolaryngol (Stockh) 1989; Suppl 467: 1–279.
16. Khanna SM, Keilson SE, Ulfendahl M, Teich MC. Spontaneous cellular vibrations in the guinea-pig temporal-bone preparation. Br J Audiol 1993; 27 (in press).
17. Keilson SE, Teich MC, Khanna SM, Ulfendahl M. Spontaneous vibrations of cells in the guinea-pig cochlea. In: Lim DJ, ed. Abstracts Fourteenth Midwinter Research Meeting of Association for Research in Otolaryngology (ARO). No 153. Des Moines, Iowa: ARO, 1991: 50.
18. Keilson SE, Teich MC, Khanna SM, Ulfendahl M. Comparison of frequency tuning curves and spontaneous cellular vibrations in the guinea-pig cochlea. In: Lim DJ, ed. Abstracts Fifteenth Midwinter Research Meeting of Association for Research in Otolaryngology (ARO). No 458. Des Moines, Iowa: ARO, 1992: 150.
19. Blackman R, Tukey J. The measurement of power spectra. New York: Dover, 1959.
20. Schwartz M, Shaw L. Signal processing: discrete spectral analysis, detection, and estimation. New York: McGraw-Hill, 1975.
21. Jenkins G, Watts D. Spectral analysis and its applications. San Francisco: Holden-Day, 1968.
22. Evans EF, Wilson JP, Borerwe TA. Animal models of tinnitus. In: Evered D, Lawrenson G, eds. Tinnitus. London: Pitman, 1981: 108–38.
23. Ohyama K, Wada H, Kobayashi T, Takasaka T. Spontaneous otoacoustic emissions in the guinea pig. Hear Res 1991; 56: 111–21.

24. Ohyama K, Sato T, Wada H, Takasaka T. Frequency instability of the spontaneous otoacoustic emissions in the guinea pig. In: Lim DJ, ed. Abstracts Fifteenth Midwinter Research Meeting of Association for Research in Otolaryngology (ARO). No 459. Des Moines, Iowa: ARO, 1992: 150.
25. Probst R, Lonsbury-Martin BL, Martin GK. A review of otoacoustic emissions. J Acoust Soc Am 1991; 89: 2027–67.

Manuscript received November 27, 1992; accepted January 12, 1993

Address for correspondence:
M. C. Teich
Columbia University
Department of Electrical Engineering
New York, 10027
USA